# Electrical behavior of $\beta$ -Ga<sub>2</sub>O<sub>3</sub> Schottky diodes with different Schottky metals

Yao Yao, Raveena Gangireddy, and Jaewoo KimKalyan Kumar DasRobert F. Davis and Lisa M. Porter

Citation: Journal of Vacuum Science & Technology B, Nanotechnology and Microelectronics: Materials, Processing, Measurement, and Phenomena **35**, 03D113 (2017); doi: 10.1116/1.4980042

View online: http://dx.doi.org/10.1116/1.4980042

View Table of Contents: http://avs.scitation.org/toc/jvb/35/3

Published by the American Vacuum Society





## Electrical behavior of $\beta$ -Ga<sub>2</sub>O<sub>3</sub> Schottky diodes with different Schottky metals

Yao Yao, a) Raveena Gangireddy, and Jaewoo Kim

Department of Materials Science and Engineering, Carnegie Mellon University, 5000 Forbes Avenue, Pittsburgh, Pennsylvania 15213

Kalyan Kumar Das

JBP Materials, Morrisville, North Carolina 27560

Robert F. Davis and Lisa M. Porterb)

Department of Materials Science and Engineering, Carnegie Mellon University, 5000 Forbes Avenue, Pittsburgh, Pennsylvania 15213

(Received 16 January 2017; accepted 29 March 2017; published 5 May 2017)

Schottky diodes based on  $(\bar{2}01)$   $\beta$ -Ga<sub>2</sub>O<sub>3</sub> substrates and (010)  $\beta$ -Ga<sub>2</sub>O<sub>3</sub> homoepitaxial layers were formed using five different Schottky metals: W, Cu, Ni, Ir, and Pt. Based on a comparison of the effects of different wet chemical surface treatments on the Ga<sub>2</sub>O<sub>3</sub> Schottky diodes, it was established that a treatment with an organic solvent, cleaning with HCl and H<sub>2</sub>O<sub>2</sub>, and rinsing with deionized water following each step yielded the best results. Schottky barrier heights calculated from current-voltage (I-V) and capacitance-voltage (C-V) measurements of the five selected metals were typically in the range of 1.0-1.3 and 1.6-2.0 eV, respectively, and showed little dependence on the metal work function. Several diodes also displayed inhomogeneous Schottky barrier behavior at room temperature. The results indicate that bulk or near-surface defects and/or unpassivated surface states may have a more dominant effect on the electrical behavior of these diodes compared to the choice of Schottky metal and its work function. © 2017 American Vacuum Society.

[http://dx.doi.org/10.1116/1.4980042]

#### I. INTRODUCTION

Gallium oxide (Ga<sub>2</sub>O<sub>3</sub>) is an emerging next-generation wide band gap semiconductor, having already demonstrated a variety of applications from ultrahigh efficiency electronics<sup>1-6</sup> to solar-blind ultraviolet photodetectors.<sup>7-11</sup> Ga<sub>2</sub>O<sub>3</sub> exists in five known polytypes  $(\alpha, \beta, \gamma, \delta, \text{ and } \varepsilon)$ , of which  $\beta$ -Ga<sub>2</sub>O<sub>3</sub> is the most thermodynamically stable.  $\beta$ -Ga<sub>2</sub>O<sub>3</sub> has the advantage of a larger band gap  $(\sim 4.8 \, eV)^{12-16}$  compared to other wide bandgap semiconductors such as SiC and GaN. Moreover, it is commercially available as a single crystal substrate produced from the melt, <sup>17</sup> making it more economically feasible for future large-scale adoption. The large bandgap of  $\beta$ -Ga<sub>2</sub>O<sub>3</sub> allows it to handle large electric fields, which in turn gives it Baliga's figure-of-merit for power devices that is ten and four times larger than that of SiC and GaN, respectively. 18,19

Table I summarizes the current literature on Schottky barrier diodes based on Ga<sub>2</sub>O<sub>3</sub>. The different device structures, preparation methods, and substrate orientations among these different studies make direct comparisons difficult. In the present study, to first establish a cleaning method for subsequent metallization, we conducted a comparison of five selected wet chemical cleaning treatments.

After establishing a surface cleaning treatment, we characterized the electrical behavior, via I-V and C-V measurements, of Schottky diodes with five different Schottky metals (W, Cu, Ni, Ir, and Pt). Schottky barrier heights (SBHs) were calculated from the measurements and are discussed in terms of predicted behavior according to the Schottky–Mott relation, which predicts that the SBH  $(\Phi_B)$ equals the difference between the electron affinity ( $\chi_S$ ) of the semiconductor and the work function of the metal  $(\Phi_M)^{31}$ 

$$\Phi_B = \Phi_M - \chi_S. \tag{1}$$

The five selected metals represent a range of work functions from moderate to high.

#### II. EXPERIMENT

All bulk substrates used in this work were pieces cut from 2-in. diameter, *n*-type ( $\bar{2}01$ )  $\beta$ -Ga<sub>2</sub>O<sub>3</sub> wafers grown using the edge-defined film fed growth (EFG) method and purchased from Tamura Corporation, Japan. The substrates were grown with Sn as an in situ dopant, at a concentration of  $5-8 \times 10^{18} \,\mathrm{cm}^{-3}$ . An image of the  $\beta$ -Ga<sub>2</sub>O<sub>3</sub> substrate is shown in Fig. 1(a). Epilayers of unintentionally doped  $Ga_2O_3$  on *n*-type (010)  $\beta$ - $Ga_2O_3$  were also used in this study; these were grown using metalorganic chemical vapor deposition by Novel Crystal Technology, Inc., in Japan.

A few reports on surface cleaning methods used for Schottky contacts to  $\beta$ -Ga<sub>2</sub>O<sub>3</sub> include buffered oxide etch (BOE), <sup>10</sup> HF (46%) followed by Piranha etch  $(H_2SO_4 + H_2O_2)^{22}$  and Piranha etch  $(H_2SO_4 + 30\% H_2O_2 1:1)$  followed by BOE.<sup>25</sup> Piranha etch is, however, known to be highly exothermic and therefore potentially hazardous. Based on common practice for surface treatment in other semiconductor systems, we selected three acid etchants (10% dilute HCl, BOE, and 10% dilute HF) as possible candidates in our cleaning treatment

a)Electronic mail: yyao1@andrew.cmu.edu

b) Author to whom correspondence should be addressed; electronic mail: lporter@andrew.cmu.edu

Table I. Summary of Schottky contacts to  $Ga_2O_3$  reported in the literature. Abbreviations used are given as follows. FZ = floating zone growth, PLD = plasma laser deposition, CZ = Czochralski method growth, PES = photoemission spectroscopy, EFG = edge-defined film-fed growth, IPE = internal photoemission, UID = unintentionally doped, and HVPE = halide vapor phase epitaxy.

Substrate				Schottky barrier	
Growth [doping Conc. (cm <sup>-3</sup> )]	Orientation	Cleaning method	Metal	Barrier height $\phi_B$ (eV)	Ideality factor n
FZ single crystal (10 <sup>17</sup> –10 <sup>18</sup> ) (Ref. 10)	(100)	Solvent, BOE	Au	1.2-~1.1 ( <i>I-V</i> )	1.8–1.1
CZ single crystal (UID $0.6-8 \times 10^{17}$ ) (Ref. 20)	(100)	NR	Au	0.98 (I-V) $1.01 \pm 0.05 (PES)$	1.09
CZ single crystal (UID 0.6–8 $\times$ 10 <sup>17</sup> ) (Ref. 21)	(100)	Cleaved surface	Ni	0.97 ( <i>I-V</i> ) 1.22 ( <i>C-V</i> )	-
FZ single crystal (UID $3-5 \times 10^{16}$ ) (Ref. 22)	(010)	Solvent, HF, piranha	Pt	1.46–1.47 ( <i>I-V</i> ) 1.52 ( <i>C-V</i> )	1.04–1.06
EFG single crystal (UID $1.1 \times 10^{17}$ ) (Ref. 23)	(010)	BCl <sub>3</sub> for ohmic contacts	Ni	1.49 ( <i>I-V</i> ) 1.55 ( <i>C-V</i> ) 1.55 (IPE)	1.04
2 $\mu$ m undoped homoepitaxial layer on <i>n</i> -type ( $\sim$ 4.1 $\times$ 10 <sup>18</sup> ) (Ref. 24)	(010)	NR	Ni	0.95–1.01 ( <i>I-V</i> )	3.38–1.21
EFG single crystal $(2.8 \times 10^{17})$ (Ref. 25)	$(\bar{2}01)$	Solvent, piranha, BOE	Ni	1.08 ( <i>I-V</i> ) 1.12 ( <i>C-V</i> )	1.19
EFG single crystal ( $\sim$ 1.7 × 10 <sup>17</sup> ) (Ref. 26)	(201)	NR	Ni	1.05 ( <i>I-V</i> ) 1.2 ( <i>C-V</i> )	_
EFG single crystal (UID $1.2 \times 10^{17}$ ) (Ref. 27)	(201)	NR	Ni	1.25 ( <i>I-V</i> ) 1.18 ( <i>C-V</i> )	1.01
EFG single crystal $(3.9 \times 10^{18})$ (Ref. 28)	$(\bar{2}01)$	NR	Ni	0.9 ( <i>I-V</i> ) 1.49 ( <i>C-V</i> )	1.4
PLD epi/ZnO/sapphire $(1.6 \times 10^{18})$ (Ref. 29)	$(\bar{2}01)$	NR	Cu	0.92 (I-V)	1.22
HVPE epi/sapphire $(1.2 \times 10^{16})$ (Ref. 30)	(001)	Solvent and acid. BCl <sub>3</sub> for ohmic contacts	Pt	1.15 ( <i>I-V</i> ) 1.12 ( <i>C-V</i> )	~1

study. However, HF was discontinued because it was observed to adversely affect the photoresist used for photolithography. As shown in Fig. 1(b), after 5 min of soaking, HF began to etch through the photoresist. Since  $H_2O_2$  has been reported to improve rectifying behavior in Schottky contacts to  $ZnO_1^{32}$  we included  $H_2O_2$  in our surface treatment study.

In total, we investigated five different wet chemical cleaning treatments. Each substrate was first degreased by sequentially sonicating in (1) acetone, isopropanol, and deionized (DI) water. Samples that received acid treatment were followed by (2) HCl, (3) BOE, (4) HCl and H<sub>2</sub>O<sub>2</sub>, or (5) BOE and H<sub>2</sub>O<sub>2</sub>. For HCl cleaning, samples were soaked in 10% HCl for 5 min at room temperature and rinsed with DI water. For BOE cleaning, samples were soaked in BOE for 5 min at

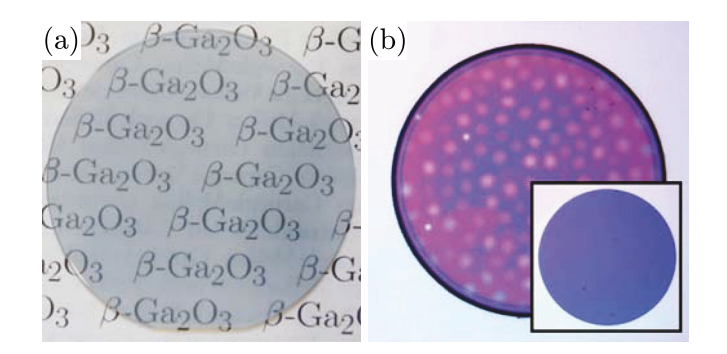


Fig. 1. (Color online) (a) Image of an n-type ( $\bar{2}01$ )  $\beta$ -Ga<sub>2</sub>O<sub>3</sub> wafer. The wafer is transparent with a slight blue tint due to Sn doping. (b) Optical image of the photoresist after 5 min of HF soaking. The inset shows the photoresist before HF soaking.

room temperature and rinsed with DI water. For  $H_2O_2$  cleaning, samples were soaked for 5 min in boiling  $H_2O_2$  at 85 °C and rinsed with DI water. All the samples were blow dried in nitrogen after each DI water rinse.

Ti/Au (20 nm/100 nm) ohmic contacts were formed by electron-beam evaporation (base pressure:  $1-5 \times 10^{-9}$  Torr) onto unheated substrates and postannealing in flowing Ar at 400 °C for 1 min. These metal stack and annealing conditions were found to produce the most reliable and consistent ohmic behavior. Anneals were performed in a quartz tube in a resistively heated furnace. Schottky metals were also deposited by electron beam evaporation onto unheated substrates. Ni (50 nm) was used to form Schottky contacts for the surface treatment study. The rectifying Schottky behavior of W, Cu, Ni, Ir, and Pt on β-Ga<sub>2</sub>O<sub>3</sub> cleaned with HCl and H<sub>2</sub>O<sub>2</sub> was then investigated. The HCl and H<sub>2</sub>O<sub>2</sub> surface treatment was based on findings from our surface cleaning study.

Schottky diodes were prepared with two different device structures. One consists of a lateral structure, in which both the ohmic and Schottky contacts are formed on the top side of the substrate. In this structure, the Schottky contacts are circular dots with a diameter of  $200 \, \mu \text{m}$ , separated from the ohmic contacts by  $100 \, \mu \text{m}$ . The contacts were patterned using a conventional photolithography lift-off method.

The other structure consisted of a vertical structure. In these devices, the ohmic contact covered the entire back side of the device. Schottky diodes were formed using a contact shadow mask on the top side of the substrate. The shadow

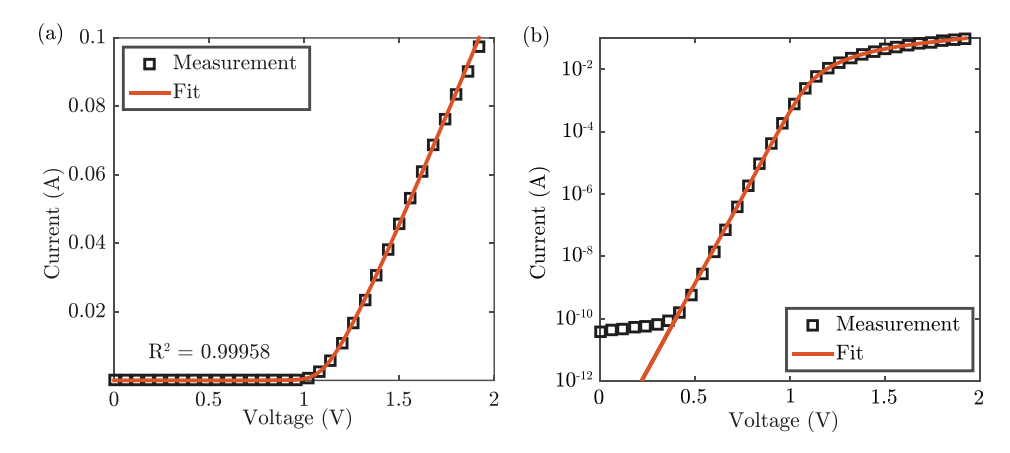


Fig. 2. (Color online) Forward current–voltage (I-V) characteristics of a Ni on the bulk  $Ga_2O_3(\bar{2}01)$  vertical Schottky diode (diameter  $125 \,\mu m$ ) on the (a) linear and (b) log scale.

mask consists of holes with four different diameters (500, 250, 125, and 62.5  $\mu$ m).

The lateral device structure was initially chosen to allow the comparison of diode behavior between the bulk and the epitaxial films; the latter require lateral structures if grown on an insulating substrate. Samples for the cleaning study were all fabricated using the lateral structure. More than 50 diodes were prepared on each sample for statistical analysis. Approximately 100 Ni and Cu diodes were fabricated using the vertical device structure, primarily to minimize leakage currents due to edge effects present in lateral device structures.

All current–voltage (*I-V*) measurements were performed using an Agilent 4155C Semiconductor Parameter Analyzer and a Signatone S-1060H-4QR probe station. Capacitance–voltage (*C-V*) measurements were performed using an HP 4284A LCR meter.

#### III. RESULTS

For rectifying contacts, the current–voltage (I-V) behavior is described by the thermionic emission equation

$$I = I_s \exp\left[\frac{q(V - IR_s)}{nk_BT} - 1\right],\tag{2}$$

where q is the electron charge,  $R_s$  is the series resistance, n is the ideality factor,  $k_B$  is the Boltzmann constant, T is the temperature, and  $I_s$  is the saturation current given by

$$I_s = AA^{**}T^2 \exp\left(-\frac{q\phi_B}{k_B T}\right),\tag{3}$$

where *A* is the contact area,  $A^{**}$  is the Richardson constant, and  $\phi_B$  is the Schottky barrier height. For  $\beta$ -Ga<sub>2</sub>O<sub>3</sub>, using the electron effective mass  $m^* = 0.28m_0$ , <sup>16</sup> we calculate the Richardson constant to be 33.65 A/(cm K)<sup>2</sup>.

Figure 2 shows an example of a typical I-V behavior of a vertical Ni Schottky diode on  $(\bar{2}01)$  Ga<sub>2</sub>O<sub>3</sub>. The current increases exponentially with applied voltage until the series resistance begins to dominate, corresponding to the saturation region in the log I vs V plot.

The ideality factor n, Schottky barrier height  $\phi_B$ , and series resistance  $R_s$  values were calculated using the method

described by Cheung and Cheung.<sup>34</sup> These values were then used to calculate a fitted line to the measured data. An R-squared coefficient of determination ( $R^2$ ) is calculated to determine the goodness of fit. Only data with  $R^2 > 0.98$  were selected for the subsequent analysis. Data whose fit did not meet the  $R^2$  criterion generally correspond to data that did not follow the thermionic emission model, possibly due to the presence of interfacial defects. This will be discussed later in this paper.

Table II shows a summary of results of Ni/Ga $_2O_3$  lateral Schottky diodes from the five different cleaning methods. The calculated Schottky barrier heights, which range between 0.87 and 0.94 eV, are at the lower end but within the range of values reported in the literature (Table I).

Each of the acid treatments yielded diodes with lower ideality factors, higher Schottky barrier heights, and lower series resistances than those treated with organic solvents only. Of these four treatments, the samples cleaned with HCl and  $\rm H_2O_2$  exhibited the highest barrier heights and lowest series resistances of any of the treatments, therefore demonstrating the most improvement in diode characteristics. The large variation in leakage current density is attributed to edge effects and defects, as discussed later. Figures 3(a) and 3(b) show a comparison of barrier height versus ideality factor and series resistance for the five types of samples.

Based on the results presented above, all the Ga<sub>2</sub>O<sub>3</sub> Schottky diodes in our subsequent studies were pretreated using HCl and H<sub>2</sub>O<sub>2</sub>. The Schottky diodes reported below were fabricated with metals (W, Cu, Ni, Ir, and Pt) having a

Table II. Summary of the results from I-V measurements of Ni lateral Schottky diodes (diameter 200  $\mu$ m) on ( $\bar{2}01$ )  $\beta\text{-}Ga_2O_3$  pretreated with different wet chemicals.

Method	$\phi_B$ (eV)	n	$R_{s}\left(\Omega\right)$	Leakage current density at -5 V (A/cm <sup>2</sup> )
Organic	$0.87 \pm 0.01$	$1.40 \pm 0.06$	$3.73 \times 10^{6}$	$0.60 \pm 0.28$
HCl	$0.89 \pm 0.01$	$1.26 \pm 0.05$	$9.06 \times 10^{5}$	$0.84 \pm 0.29$
BOE	$0.89 \pm 0.01$	$1.26 \pm 0.02$	$2.03\times10^{5}$	$1.12 \pm 0.20$
HCl and H <sub>2</sub> O <sub>2</sub>	$0.94 \pm 0.01$	$1.30 \pm 0.02$	$6.94 \times 10^{2}$	$0.63 \pm 0.20$
BOE and H <sub>2</sub> O <sub>2</sub>	$0.90 \pm 0.01$	$1.37 \pm 0.03$	$2.30\times10^3$	$1.37 \pm 0.20$

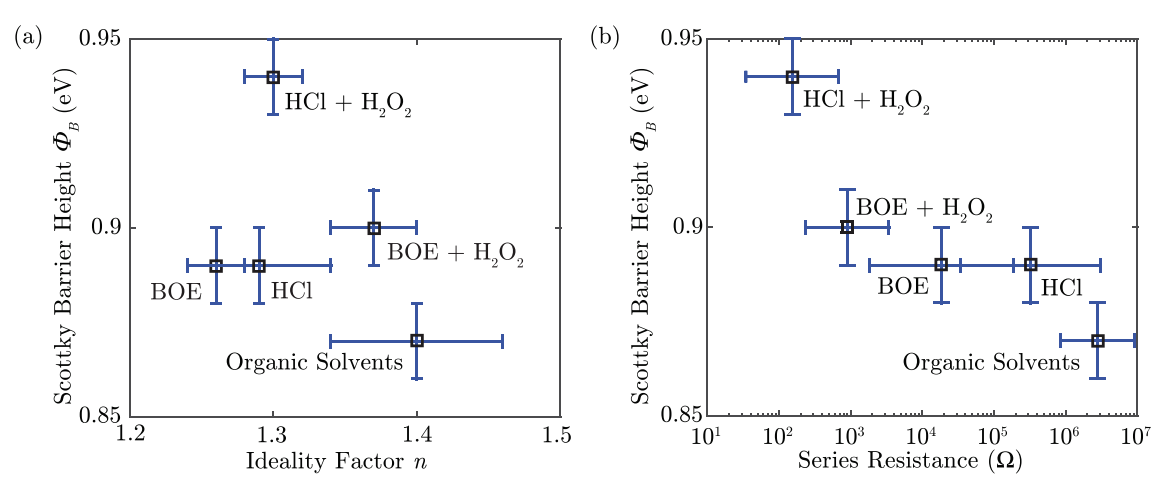


Fig. 3. (Color online) Schottky barrier height vs (a) ideality factor and (b) series resistance for diodes pretreated using different wet chemicals.

range of work functions. Devices with both lateral and vertical structures were fabricated, on both ( $\bar{2}01$ ) single crystal bulk substrates and (010) epitaxial films.

In addition to current–voltage measurements as described previously, capacitance–voltage measurements were conducted on many of the diodes. Under reverse bias, the depletion region at the metal-semiconductor interface acts as a capacitor. For an n-type semiconductor with permittivity  $\varepsilon_s$  and electron concentration  $N_d$ , its depletion width is given by

$$W_D = \sqrt{\frac{2\varepsilon_s}{qN_d} \left(\psi_{bi} - V - \frac{k_B T}{q}\right)},\tag{4}$$

where  $\psi_{bi}$  is the built-in voltage of the diode. Capacitance can therefore be expressed as

$$C = \frac{A\varepsilon_s}{W_D} = A\sqrt{\frac{q\varepsilon_s N_d}{\psi_{bi} - V - k_B T/q}},$$
 (5)

or

$$\frac{1}{C^2} = \frac{2(\psi_{bi} - V - k_B T/q)}{A^2 q \varepsilon_s N_d}.$$
 (6)

Therefore,  $\psi_{bi}$  and  $N_d$  can be calculated from the intercept and the slope, respectively, of a plot of  $1/C^2$  vs V. The Schottky barrier height is related to the built-in voltage and carrier concentration by

$$\phi_B = \psi_{bi} + \phi_n + \frac{k_B T}{q},\tag{7}$$

$$\phi_n = E_C - E_F = k_B T \ln \frac{N_c}{N_d},\tag{8}$$

where  $E_C$  is the conduction band minimum,  $E_F$  is the Fermi level, and  $N_c$  is the effective density of states in the conduction band

$$N_c = 2\left(\frac{2\pi m^* k_B T}{h^2}\right)^{3/2}. (9)$$

Table III lists the Schottky barrier heights and ideality factors calculated from I-V and C-V measurements. The results according to the Schottky metal, device structure (lateral versus vertical), and whether the diode is directly on a  $(\bar{2}01)$  substrate or a (010) substrate with an epitaxial layer are listed in Table III. The Schottky barrier heights are

Table III. Summary of electrical measurements of  $Ga_2O_3$  Schottky diodes with different Schottky metals. The "bulk" substrates are ( $\bar{2}01$ ) oriented; the "epi" films are (010) oriented.

Metal	Work function $\phi_M$ (eV) (Ref. 35)	Structure	Substrate	I- $V$		C- $V$
				$\phi_B$ (eV)	n	$\phi_B$ (eV)
W	4.55	Lateral	Bulk	$0.91 \pm 0.09$	$1.40 \pm 0.4$	$1.94 \pm 0.1$
		Lateral	Epi	$1.05 \pm 0.03$	$2.68 \pm 0.3$	
Cu	4.65	Vertical	Bulk	$1.13 \pm 0.1$	$1.53 \pm 0.2$	
Ni 5.1	5.15	Lateral	Bulk	$1.04 \pm 0.02$	$1.33 \pm 0.03$	$1.61 \pm 0.1$
		Lateral	Epi	$1.08 \pm 0.1$	$1.68 \pm 0.4$	
		Vertical	Bulk	$1.00 \pm 0.06$	$1.57 \pm 0.2$	
Ir	5.27	Lateral	Bulk	$1.29 \pm 0.1$	$1.45 \pm 0.2$	$2.3 \pm 0.4$
		Lateral	Epi	$1.40 \pm 0.08$	$1.64 \pm 0.2$	
Pt	5.65	Lateral	Bulk	$1.05 \pm 0.03$	$1.40 \pm 0.04$	$1.9 \pm 0.1$
		Lateral	Epi	$1.34 \pm 0.1$	$1.87 \pm 0.3$	

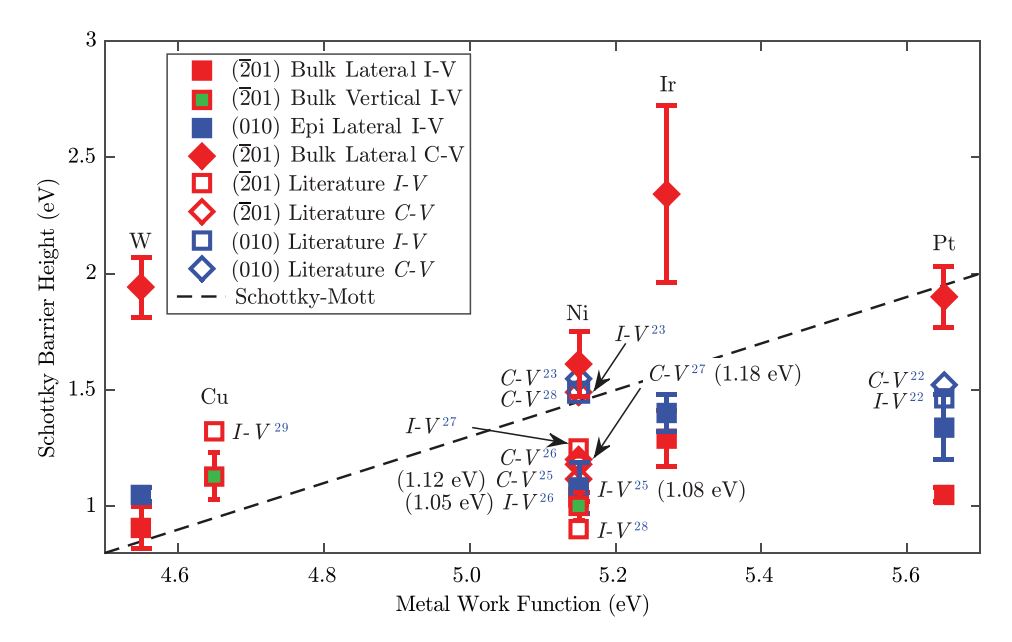


Fig. 4. (Color online) Calculated Schottky barrier heights vs metal work function for Schottky diodes on  $(\bar{2}01)$  bulk and (010) epitaxial  $\beta$ -Ga<sub>2</sub>O<sub>3</sub>. Schottky barrier height values on  $(\bar{2}01)$  Ga<sub>2</sub>O<sub>3</sub> as reported in the literature are also included for comparison. The Schottky–Mott predicted line is calculated based on the Schottky–Mott relation [Eq. (1)], calculated assuming an electron affinity of 3.7 eV (Ref. 37).

plotted as a function of the Schottky metal work function in Fig. 4.

With reference to the lateral structure devices, we observed that the barrier height values on the (010) epitaxial layer were consistently higher than those on the ( $\bar{2}01$ ) bulk substrate. This is consistent with other reports in the literature that reported higher barrier heights for (010) oriented substrates versus ( $\bar{2}01$ ) oriented substrates (see Table I). Our calculated barrier heights on ( $\bar{2}01$ ) bulk substrates are within the range of values reported in the literature, while those on the (010) epitaxial film tend to be lower than reported values.

It is noted that the barrier height values calculated from C-V measurements in each case were significantly higher than the respective I-V determined values. It is normal for C-V determined barrier heights to be higher than I-V determined barrier heights, particularly due to the presence of barrier inhomogeneity in a nonideal diode. It is therefore expected that the I-V values in this study are underestimated due to the fact that the ideality factors are >1.0. Inhomogeneous Schottky barriers and their effect on the electrical behavior of  $Ga_2O_3$  diodes are discussed in more detail in Sec. IV.

## IV. DISCUSSION

There are a few important observations we can make in this study. First, as mentioned above, the I-V determined barrier heights are significantly lower than the C-V determined barrier heights (Table III and Fig. 4). It is expected that the C-V determined values are more accurate in terms of an areal average Schottky barrier within each diode; however, the I-V determined values should be more representative of the effective Schottky barrier heights for current flow. The non-ideal (n > 1.0) behavior is attributed to defects in  $Ga_2O_3$ ,

which act as low-barrier regions that yield inhomogeneous Schottky diodes.

For example, in vertical device structures, a significant percentage of diodes displayed two distinct linear regions at room temperature in plots of  $\log I$  vs V, as shown in Fig. 5.

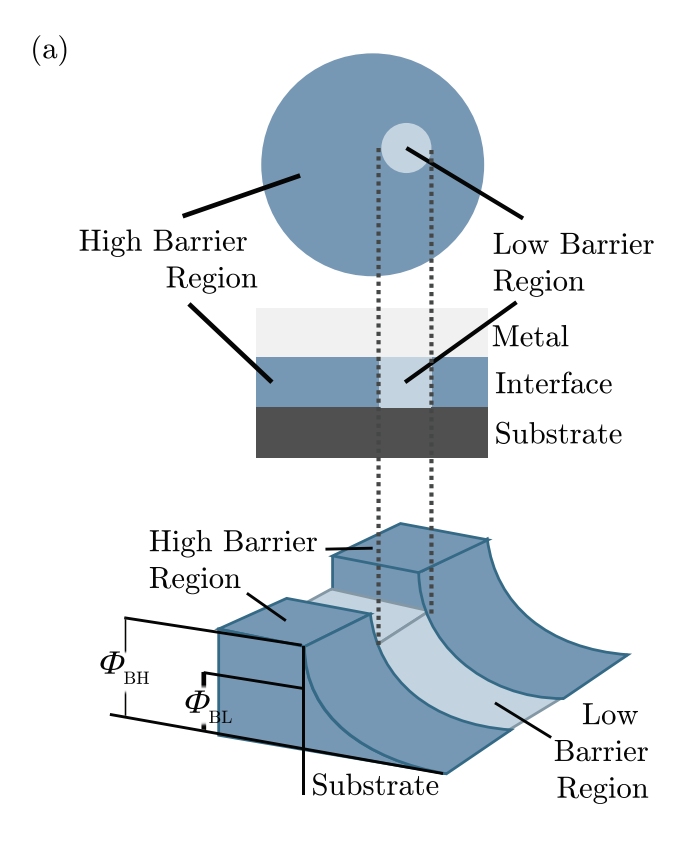
This double barrier behavior can be modeled as two diodes in parallel, one with a high barrier height and the other with a low barrier height. The total current through the contact would be the sum of currents through the high and low barrier patches<sup>38</sup>

$$I = I_{sat}^{H} \exp\left[\frac{q(V - IR_{s}^{H})}{n^{H}kT}\right] + I_{sat}^{L} \exp\left[\frac{q(V - IR_{s}^{L})}{n^{L}kT}\right], \quad (10)$$

where the superscripts H and L denote the high and low barrier regions, respectively.

In this case, the low barrier region was found to have a Schottky barrier of  $0.8 \pm 0.06\,\mathrm{eV}$ . As evidence that this behavior is associated with defects in the material, it was observed that the percentage of diodes displaying double barrier behavior (as shown in Fig. 5) increased as the diode area increased (Fig. 6), i.e., the larger the contact size is, the more likely it is for the diode to exhibit a double barrier behavior since it is more likely to overlap with an area containing defects. This is statistically significant because the number of devices for each choice of contact size and metal is between 30 and 80.

Another important observation from this study is that neither *I-V* nor *C-V* determined Schottky barrier height values showed a strong correlation with the work functions of the metals (Fig. 4). The slopes of the least-squares line fits to the "bulk lateral *I-V*," "epilateral *I-V*," and "bulk lateral *C-V*," sets of data were 0.18, 0.29, and 0.16, respectively. The "bulk vertical *I-V*," which has only two data points, actually has a slight negative slope (–0.18). In comparison



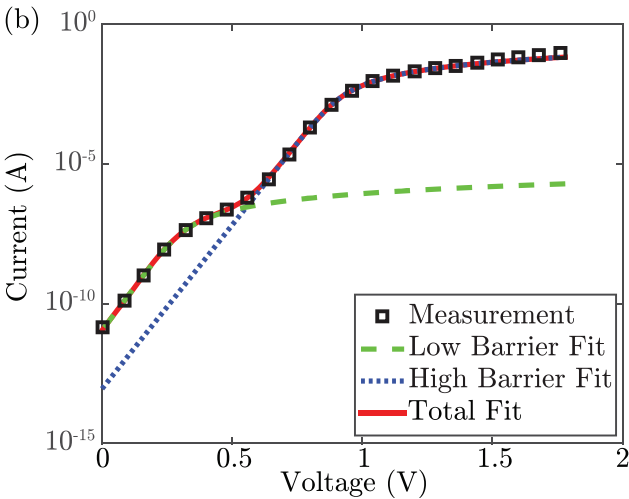


Fig. 5. (Color online) (a) Schematic of a diode with two distinct barrier regions. (b) Log I vs V plot of a Ni/Ga<sub>2</sub>O<sub>3</sub> Schottky diode at room temperature showing two linear regions, modeled as two regions of different barrier heights.

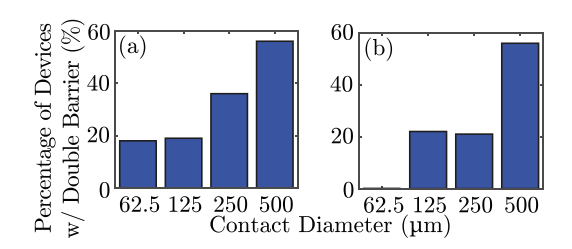


Fig. 6. (Color online) Percentage of devices showing double barrier behavior at room temperature for (a) Ni and (b) Cu as a function of the contact size. The total number of devices is between 30 and 80 for each choice of contact size and metal.

with the Schottky–Mott [Eq. (1)] predicted behavior (dashed line in Fig. 4) for an ideal diode, these results indicate that factors other than the metal work function dominate the Schottky behavior in the  $Ga_2O_3$  diodes reported here.

One of the dominant effects on the Schottky diode behavior is likely due to defects in the bulk and/or near the surface region of Ga<sub>2</sub>O<sub>3</sub>. The inhomogeneous behavior displayed in Fig. 5 and the effect of the contact area (Fig. 6) suggest that defects within the Ga<sub>2</sub>O<sub>3</sub> play an important role.

Another strong effect may come from the presence of surface states at a defective, nonstoichiometric, and/or unpassivated  $Ga_2O_3$  surface. Although the HCl and  $H_2O_2$  surface pretreatment resulted in improved diode characteristics (e.g., higher Schottky barrier heights and lower series resistance, refer to Table II and Fig. 3) relative to the other cleaning treatments investigated, the ideality factors were still >1.0, which indicates less-than-ideal behavior.

Previous work on ZnO suggests that  $H_2O_2$  treatment yields an O-rich surface and lowers the oxygen vacancy concentration near the surface.<sup>39</sup> Oxygen vacancies, which are deep level defects in ZnO, are suspected to pin the Fermi level. It has been observed that  $H_2O_2$  treatment increases the Schottky barrier height on ZnO (Ref. 32) in correspondence with an upward band bending at the surface of ZnO.<sup>32</sup> Similar effects from  $H_2O_2$  might be expected in  $Ga_2O_3$ , where oxygen vacancies are also predicted to be deep level defects.<sup>14</sup> Upward band bending has also been proposed in  $\beta$ -Ga<sub>2</sub>O<sub>3</sub> for the reduction of carrier concentration on annealing in oxygen rich atmospheres.<sup>40</sup>

The results from this study indicate that the treatment of the Ga<sub>2</sub>O<sub>3</sub> surface with HCl and H<sub>2</sub>O<sub>2</sub> is beneficial but likely insufficient to create an ideal surface for device fabrication. Further investigation is needed to determine if additional surface treatment steps [e.g., dry etching using BCl<sub>3</sub> (Ref. 41)] could be combined with these wet chemicals to remove surface damage and yield a more ideal surface.

### **V. SUMMARY**

In this study, we compared the effects of five different wet chemical treatments on the electrical behavior (e.g., barrier heights and ideality factors) of Ni/( $\bar{2}01$ )  $\beta$ -Ga<sub>2</sub>O<sub>3</sub> Schottky diodes. Pretreatment with organic solvents followed by HCl, H<sub>2</sub>O<sub>2</sub>, and DI water was found to yield the most favorable characteristics. Schottky diodes with five different Schottky metals (W, Cu, Ni, Ir, and Pt) were fabricated using the HCl and H<sub>2</sub>O<sub>2</sub> pretreatment and characterized using I-V and C-V measurements. Schottky barrier heights were calculated from the measurements and found to have little correlation with the metal work functions. It was concluded that bulk or near-surface defects and/or surface states have a dominant effect on the electrical behavior. The results point to the need for further investigations on the types of defects in Ga<sub>2</sub>O<sub>3</sub> and how to prepare a more ideal surface for device structures.

#### **ACKNOWLEDGMENTS**

The authors acknowledge partial support for this research from the National Science Foundation through NSF Grant No. ECCS-1642740. The use of the Materials Characterization Facility at Carnegie Mellon University was supported by Grant No. MCF-677785.

- <sup>1</sup>K. Matsuzaki, H. Hiramatsu, K. Nomura, H. Yanagi, T. Kamiya, M. Hirano, and H. Hosono, Thin Solid Films **496**, 37 (2006).
- <sup>2</sup>M. Higashiwaki, K. Sasaki, A. Kuramata, T. Masui, and S. Yamakoshi, Appl. Phys. Lett. 100, 013504 (2012).
- <sup>3</sup>K. Sasaki, M. Higashiwaki, A. Kuramata, T. Masui, and S. Yamakoshi, J. Cryst. Growth **378**, 591 (2013).
- <sup>4</sup>M. Higashiwaki, K. Sasaki, T. Kamimura, M. H. Wong, D. Krishnamurthy, A. Kuramata, T. Masui, and S. Yamakoshi, Appl. Phys. Lett. **103**, 123511 (2013).
- <sup>5</sup>M. Higashiwaki, K. Sasaki, M. H. Wong, T. Kamimura, D. Krishnamurthy, A. Kuramata, T. Masui, and S. Yamakoshi, *International Electron Devices Meeting*, Washington, DC (IEEE, 2013), p. 28.7.
- <sup>6</sup>M. H. Wong, K. Sasaki, A. Kuramata, S. Yamakoshi, and M. Higashiwaki, IEEE Electron Device Lett. **37**, 212 (2016).
- <sup>7</sup>Y. Kokubun, K. Miura, F. Endo, and S. Nakagomi, Appl. Phys. Lett. **90**, 031912 (2007).
- <sup>8</sup>T. Oshima, T. Okuno, and S. Fujita, Jpn. J. Appl. Phys., Part 1 **46**, 7217 (2007).

  <sup>9</sup>T. Oshima, T. Okuno, N. Assi, N. Sazaki, S. Oshima and S. Fajita, Appl.
- <sup>9</sup>T. Oshima, T. Okuno, N. Arai, N. Suzuki, S. Ohira, and S. Fujita, Appl. Phys. Express 1, 011202 (2008).
- <sup>10</sup>R. Suzuki, S. Nakagomi, Y. Kokubun, N. Arai, and S. Ohira, Appl. Phys. Lett. **94**, 222102 (2009).
- <sup>11</sup>R. Suzuki, S. Nakagomi, and Y. Kokubun, Appl. Phys. Lett. **98**, 131114 (2011).
- <sup>12</sup>H. Tippins, Phys. Rev. **140**, A316 (1965).
- <sup>13</sup>M. Orita, H. Ohta, M. Hirano, and H. Hosono, Appl. Phys. Lett. **77**, 4166 (2000).
- <sup>14</sup>J. Varley, J. Weber, A. Janotti, and C. Van de Walle, Appl. Phys. Lett. **97**, 142106 (2010).
- <sup>15</sup>C. Janowitz et al., New J. Phys. 13, 085014 (2011).
- <sup>16</sup>H. Peelaers and C. G. Van de Walle, Phys. Status Solidi B **252**, 828 (2015).
- <sup>17</sup>Tamura Corporation, "Single-crystal gallium oxide substrates," http://www.tamura-ss.co.jp/en/products/gao/index.html accessed 6 August 2016.

- <sup>18</sup>B. Baliga, J. Appl. Phys. **53**, 1759 (1982).
- <sup>19</sup>M. Higashiwaki, K. Sasaki, A. Kuramata, T. Masui, and S. Yamakoshi, Phys. Status Solidi A 211, 21 (2014).
- <sup>20</sup>M. Mohamed, K. Irmscher, C. Janowitz, Z. Galazka, R. Manzke, and R. Fornari, Appl. Phys. Lett. **101**, 132106 (2012).
- <sup>21</sup>K. Irmscher, Z. Galazka, M. Pietsch, R. Uecker, and R. Fornari, J. Appl. Phys. **110**, 063720 (2011).
- <sup>22</sup>K. Sasaki, M. Higashiwaki, A. Kuramata, T. Masui, and S. Yamakoshi, IEEE Electron Device Lett. 34, 493 (2013).
- <sup>23</sup>Z. Zhang, E. Farzana, A. Arehart, and S. Ringel, Appl. Phys. Lett. 108, 052105 (2016).
- <sup>24</sup>S. Oh, G. Yang, and J. Kim, ECS J. Solid State Sci. Technol. 6, Q3022 (2017).
- <sup>25</sup> A. Jayawardena, A. C. Ahyi, and S. Dhar, Semicond. Sci. Technol. 31, 115002 (2016).
- <sup>26</sup>A. M. Armstrong, M. H. Crawford, A. Jayawardena, A. Ahyi, and S. Dhar, J. Appl. Phys. **119**, 103102 (2016).
- Appl. Hrys. 119, 105102 (2010).
   T. Oishi, Y. Koga, K. Harada, and M. Kasu, Appl. Phys. Express 8, 031101 (2015).
- <sup>28</sup>T. Oishi, K. Harada, Y. Koga, and M. Kasu, Jpn. J. Appl. Phys., Part 1 55, 030305 (2016).
- <sup>29</sup>D. Splith, S. Müller, F. Schmidt, H. Von Wenckstern, J. J. van Rensburg, W. E. Meyer, and M. Grundmann, Phys. Status Solidi A 211, 40 (2014).
- <sup>30</sup>M. Higashiwaki *et al.*, Appl. Phys. Lett. **108**, 133503 (2016).
- <sup>31</sup>S. M. Sze and K. K. Ng, *Physics of Semiconductor Devices*, 3rd ed. (Wiley, New Jersey, 2007).
- <sup>32</sup>L. J. Brillson and Y. Lu, J. Appl. Phys. **109**, 121301 (2011).
- <sup>33</sup>Y. Yao, R. F. Davis, and L. M. Porter, J. Electron. Mater. **46**, 2053 (2017)
- <sup>34</sup>S. K. Cheung and N. W. Cheung, Appl. Phys. Lett. **49**, 85 (1986).
- <sup>35</sup>D. R. Lide, CRC Handbook of Chemistry and Physics, 77th ed. (CRC, New York, 1996).
- <sup>36</sup>J. H. Werner and H. H. Güttler, J. Appl. Phys. **69**, 1522 (1991).
- <sup>37</sup>M. Grodzicki, P. Mazur, S. Zuber, J. Brona, and A. Ciszewski, Appl. Surf. Sci. 304, 20 (2014).
- <sup>38</sup>B. Skromme, E. Luckowski, K. Moore, M. Bhatnagar, C. Weitzel, T. Gehoski, and D. Ganser, J. Electron. Mater. 29, 376 (2000).
- <sup>39</sup>Q. Gu et al., J. Appl. Phys. **103**, 093706 (2008).
- <sup>40</sup>T. Lovejoy *et al.*, Appl. Phys. Lett. **100**, 181602 (2012).
- <sup>41</sup>L. Zhang, A. Verma, H. G. Xing, and D. Jena, Jpn. J. Appl. Phys., Part 1 56, 030304 (2017).